Effect of thermoplastic modifier variables on toughening a bismaleimide matrix resin for high-performance composite materials*

S. P. Wilkinson, T. C. Ward† and J. E. McGrath
Department of Chemistry, and The NSF Science and Technology Center — High Performance Polymeric Adhesives and Composites, Virginia Polytechnic Institute and State University, Blacksburg, VA 24061-0212, USA
(Received 6 July 1992; revised 30 July 1992)

A series of engineering thermoplastic toughness modifiers were used to modify the fracture toughness properties of a bismaleimide resin. The effects of thermoplastic loading, molecular weight and functionality were examined. Substantial improvements in K_{Ic} stress intensity values were found when modifiers possessing reactive end-groups were used. Increases in modifier molecular weight and weight per cent loading produced steady increases in K_{Ic} values and a limiting value at high concentrations and molecular weights. These observations were attributed to the thermoset network being the limiting material with respect to fracture toughness. By controlling molecular weight and adding reactive end-groups to the toughener, the fracture toughness properties of the commercial bismaleimide resin were successfully improved without sacrificing its desirable hot-melt processing characteristics. A unidirectional carbon-fibre prepreg was prepared and mode I and II fracture toughness tests were performed using double cantilever beam and end notch flexure specimens. Thermoplastic loadings of 15 and 20% of maleimide-terminated poly(ether sulphone) ($M_n = 12\,800$ g mol^{-1}) yielded composite G_{Ic} values of 489 ± 25 and 734 ± 1 J m^{-2}, respectively—a substantial improvement over the unmodified composite value of 359 ± 17 J m^{-2}.

(Keywords: fracture toughness; toughened bismaleimides; composites; functionalized polymers; high-performance resins; thermoplastic modifiers)

INTRODUCTION

A class of thermoset resins based on bismaleimide (BMI) chemistry possesses many desirable properties that are associated with thermoset networks. These include high tensile strength and modulus, excellent chemical and corrosion resistance, and good dimensional stability. A major reason for the substantial interest in bismaleimide resins at present is that they process in a manner similar to epoxies, cure without the evolution of volatiles, and exhibit higher glass transition temperatures than epoxies (approximately 230°C and above). Major applications for BMI structural composites are in military aircraft and engines.

One major disadvantage associated with many thermosetting networks is that they are inherently brittle. For BMIs to be useful as matrix resins for high-performance structural composite materials, the fracture toughness must be improved without sacrificing other important mechanical properties such as high-temperature flexural strength. One approach is to utilize engineering thermoplastics to serve as toughness modifiers for the BMI network. By controlling the molecular weight, weight per cent incorporation and end-group chemistry of the modifiers, the BMI fracture toughness may be improved while maintaining high-temperature performance and the desirable processing characteristics for hot-melt techniques. Phase separation of the thermoplastic modifier occurs during network formation. Variations in morphology associated with changes in polymer parameters such as molecular weight need to be addressed with respect to their effect upon fracture toughness properties. Recent reports[1,2] have stressed the importance of morphological control in optimizing fracture toughness. McGrail and coworkers[1] reported that a co-continuous morphology, characteristic of spinodal decomposition, resulted in optimum fracture toughness. In their case, the desired morphology was obtained by systematically varying the modifier backbone structure. In a later publication, Recker *et al.*[2] described how optimum fracture toughness was achieved by varying the weight per cent loading of modifier. At a 25% loading, a morphology that simultaneously contained both a continuous phase of thermoset and a continuous phase of thermoplastic was suggested to provide optimum toughness. These papers, owing to the proprietary nature of the work, did not completely describe the chemistry of the toughness modifiers. Hence, a desire exists to model fully these important high-performance polymeric systems, including the effect of various morphologies on mechanical properties and chemical resistance. This paper addresses how several fundamental changes to the toughness modifiers affected the morphologies and fracture toughness properties of a series of modified

* Presented at 'Advances in Polymeric Matrix Composites', 5–10 April 1992, San Francisco, CA, USA
† To whom correspondence should be addressed

0032-3861/93/040870-15

networks. The effect of morphology on chemical resistance was also studied. Existing hot-melt technology was used to prepare a unidirectional carbon-fibre prepreg that was consolidated into laminates for mechanical testing. How the matrix fracture toughness transferred into the composite material mode I and mode II fractures was of great interest. This paper addresses first the matrix materials and second the graphite composite performance.

MATRIX RESINS

EXPERIMENTAL

Materials

The commercial resin system, Matrimid 5292 A/B from Ciba Geigy (*Figure 1*), was chosen as the thermoset network to be modified with the functionalized engineering thermoplastics. This two-part system comprised 4,4'-bismaleimidodiphenylmethane (**1**) and *o,o'*-diallyl bisphenol A (**2**). In all formulations containing various thermoplastic modifiers, the ratio of **1** to **2** was kept at 57:43 parts by weight (1:0.85 mole ratio). A major reason for the choice of this resin system was the ability of component **2** to dissolve the thermoplastic modifiers, to form a hot-melt solution, and then to co-react into the network through the allyl groups without producing any volatiles.

All polymers used in this study were specifically synthesized for use as toughness modifiers to elucidate the effects of changing polymer variables on fracture toughness properties. The well documented[3,4] polymerization procedure between the diphenate salt of a bisphenol undergoing a nucleophilic aromatic substitution reaction with an activated dihalide monomer (*Figure 2*) was used to prepare a variety of amorphous thermoplastic polymers differing in backbone structure (*Figure 3*). Copolymers can be prepared by varying the types of bisphenol or dihalide monomers. The thermoplastic polyimide based on the 6F dianhydride and bisaniline A monomers was prepared using a solution imidization technique[5].

The ability of amine functional groups to react readily with an anhydride moiety was utilized to produce amine-terminated oligomers. The reaction enabled maleimide and phthalimide end-groups to be substituted on polymer chain ends, where oligomer backbone and molecular weight were kept constant. *Figure 4* outlines the reaction scheme and details the structures representing the three end-groups. Kwiatkowski and Robeson[6] first reported the synthesis of maleimide-terminated polysulphone utilizing the dimethylsulphoxide/sodium hydroxide

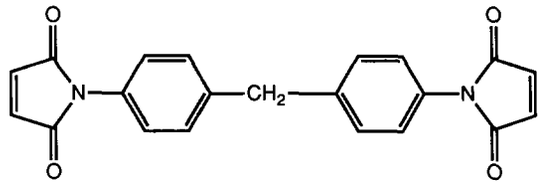

a **4,4' Bismaleimidodiphenyl methane**

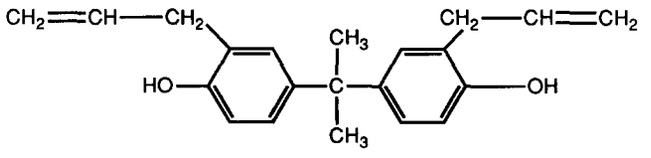

b **o,o' Diallyl Bisphenol A**

Figure 1 (a) Structure for 4,4'-bismaleimidodiphenylmethane (**1**). (b) Structure for *o,o'*-diallyl bisphenol A (**2**)

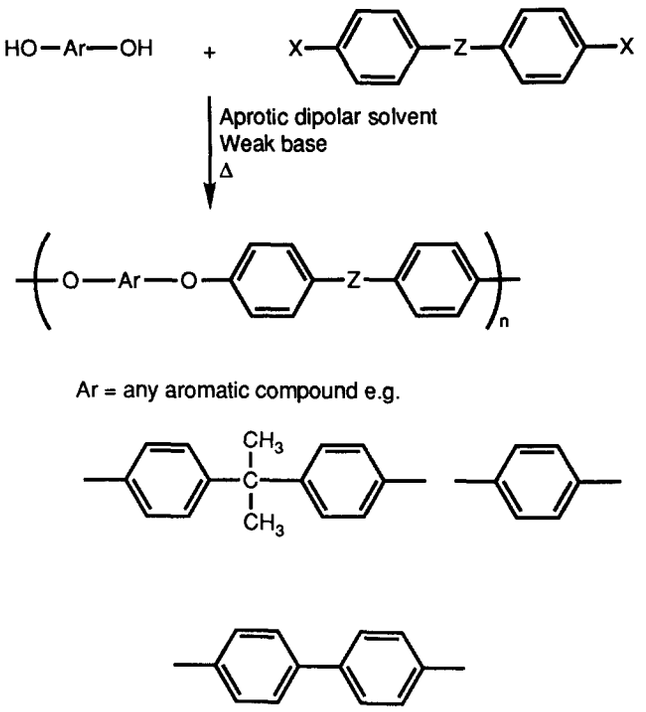

Figure 2 Nucleophilic aromatic substitution reaction for the synthesis of various poly(arylene ether)s

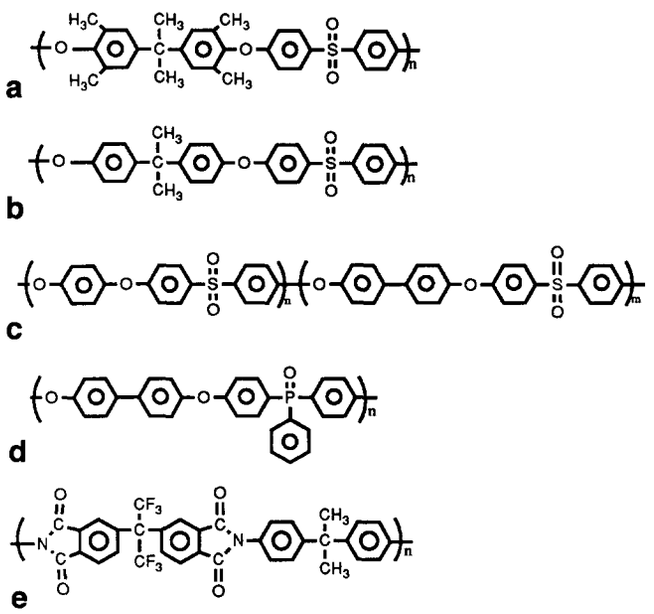

Figure 3 Amorphous thermoplastic toughness modifiers: (a) poly(arylene ether sulphone) (tetramethyl bisphenol A); (b) poly(arylene ether sulphone); (c) poly(arylene ether sulphone) copolymer; (d) poly(arylene ether phosphine oxide); (e) 6F polyimide

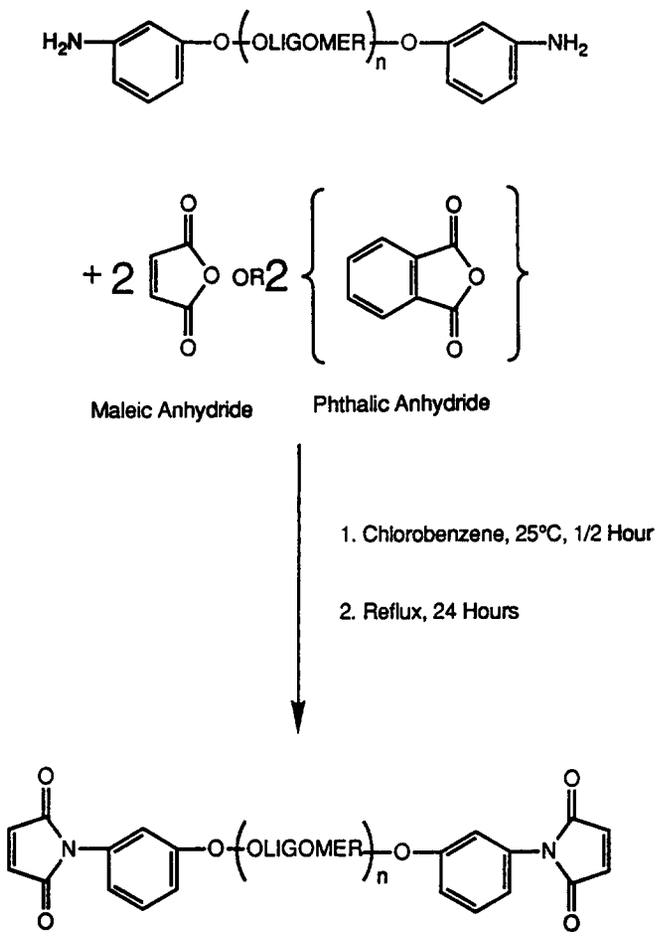

Figure 4 Schematic scheme for end-group modification

route; however, that research did not utilize the resulting polymer as a toughness modifier. Instead, their purpose was to crosslink the amorphous polymer with itself to form an insoluble, high-T_g, polymeric network possessing good thermal, mechanical and adhesive properties.

Oligomer end-capping procedure

A desired quantity of amine-terminated oligomer was dissolved in a three-necked round-bottomed flask containing chlorobenzene (15% w/v) at room temperature (heating may initially be required to dissolve all the polymer). The flask was fitted with a mechanical stirrer, thermometer and inverse Dean–Stark trap, on top of which a condenser was fitted. A 5 mol% excess of anhydride monomer (either phthalic or maleic) was added to the three-necked round-bottomed flask. The contents were stirred for 1 h at room temperature under a constant nitrogen purge, and then heated to reflux for solution imidization of the amic acid produced from the anhydride/amine reaction. After refluxing for 24 h, the solution was cooled and filtered. The polymer was precipitated from solution using a 5:1 volume ratio with methanol in excess in a high-speed blender. Upon filtering and drying the polymer, a second precipitation step was employed after redissolving the polymer in chloroform. The polymer was once again filtered and dried, and end-groups were qualitatively analysed by *FT*i.r.

Thermoplastic/thermoset hot-melt resin preparation

The diallyl bisphenol A compound **2** was initially weighed into a two-necked, round-bottomed flask. The thermoplastic modifier (preferably dried overnight in a vacuum oven) was weighed and added to the flask. A mechanical stirrer with Teflon paddle and vacuum adaptor was fitted to the flask and placed in an oil bath heated to 130°C. A vacuum was slowly applied to the stirring mixture in order to degas the resin system and remove volatiles such as residual solvent and entrapped air. Upon completing this first step, a homogeneous yellow solution was obtained. After raising the temperature to 140°C the bismaleimide resin **1** was added via a powder funnel. Again, vacuum was applied to the reaction flask with great care, and with further stirring for approximately 20 min a dark reddish brown homogeneous hot-melt solution was obtained. In this form, the hot-melt resin could be poured into silicon moulds specifically designed to the desired dimensions for fracture toughness and other specimens, or added to the resin pot within a hot-melt drum winder for fibre prepregging.

CHARACTERISTICS

Differential scanning calorimetry

To allow the diallyl derivative of bisphenol A compound (DABA) to act as a solvent for the toughness modifiers, only amorphous thermoplastics were used in this study. Glass transition temperatures for all modifiers were obtained using a DuPont 912 differential scanning calorimeter connected to a DuPont 2100 Thermal Analyst. The heating rate was 10°C min^{-1}. All reported glass transition temperatures were from the second scan, and were taken at the half-point of the slope change from the baseline. All scans were run under a nitrogen atmosphere.

Intrinsic viscosity measurements

Intrinsic viscosity measurements for the various functionalized oligomers were determined in chloroform using Cannon–Ubbelohde viscometers immersed in a water bath maintained at 25°C. Four concentrations were used for each measurement.

End-group analysis by titration

Potentiometric titrations were performed on amine-terminated oligomers[7] to compare the actual number-average molecular weight with theoretical values. This method does assume that all oligomers are 100% difunctional. In some cases, when unreacted chlorine groups were detected on a 400 MHz proton n.m.r. spectrum, the potentiometric titration method could not be used. All titrations were performed using an MCI GT-5 (COSA Instruments Corporation) automatic potentiometric titrator.

Amine-terminated oligomers were accurately weighed into a 150 ml beaker. Sample quantities were chosen to require approximately 2–4 ml of titrant, and were dissolved in 50 ml of chloroform. (Standardization of the titrant was performed using potassium hydrogen phthalate in glacial acetic acid.) Glacial acetic acid (15 ml) was slowly added with constant stirring to the chloroform solution. On complete dissolution, a titration was performed with 0.02 N anhydrous hydrogen bromide (HBr) in glacial acetic acid. End-points were determined from the maximum in the first derivative plot of the

titration curve. Reported molecular weights were based on the average from three titrations.

Dynamic mechanical thermal analysis

Dynamic mechanical thermal analysis (d.m.t.a.) was utilized to study how the thermoplastic modifiers, when incorporated into brittle thermosets, affected the storage and loss moduli. Samples were tested from −150 to 350°C with a heating rate of 1°C min^{-1}, thus exceeding both the thermoset and thermoplastic modifier glass transition temperatures. A Polymer Laboratories Mark II instrument was used at various oscillating frequencies (0.1, 0.3, 1.0, 10.0 and 20.0 Hz), with low strain amplitudes to ensure VTS co-elastic behaviour. Samples with dimensions of 3.0 mm × 6.5 mm × 30 mm were mounted in a single cantilever frame for mechanical perturbation.

K_{Ic} fracture toughness measurements

Specimen and test fixture details. The critical stress intensity factor (K_{Ic}), an indication of a material's ability to resist fracture, was measured for the thermoplastic-modified bismaleimides according to a procedure described by the American Society for Testing and Materials Specification (ASTM E399). Specimen samples were prepared by casting the degassed hot-melt resin into silicone rubber moulds possessing dimensions of 3.2 mm × 6.5 mm × 38 mm. These samples were prepared for fracture toughness testing by notching samples (approximately 0.5 mm in depth) with a reciprocating saw. The ASTM standard required that extremely sharp cracks are needed for testing purposes. The more blunt a crack is, the tougher the material appears to be, hence leading to false toughness data. Such cracks were initiated within the specimen by first cooling a razor blade in liquid nitrogen, and tapping the sharp blade within the notch using an aluminium bar. Care was taken to ensure that the crack had propagated evenly through the specimen thickness by holding the sample to the light and examining both edges.

Data reduction. Freshly cracked specimens were placed into a three-point bend apparatus, which was attached to an Instron testing machine (model 1123). The samples were tested at a crosshead speed of 50.8 mm min^{-1}. Plane strain conditions were attained as required for testing materials with the specified dimensions using the ASTM E399 standard. Upon failure, the various specimen geometries such as crack length, width and thickness were measured using digital calipers. The critical stress intensity to cause catastrophic failure in mode I crack opening was calculated using equation (3.5) from the standard test:

$$K_{Ic}=\frac{PS}{bw^{3/2}}\left[2.9\left(\frac{a}{w}\right)^{1/2}-4.6\left(\frac{a}{w}\right)^{3/2}+21.8\left(\frac{a}{w}\right)^{5/2}-37.6\left(\frac{a}{w}\right)^{7/2}+38.7\left(\frac{a}{w}\right)^{9/2}\right] \quad (1)$$

where P = load at failure, S = span length between supports, b = thickness, w = width and a = crack length. All calculated results were in MPa $m^{1/2}$. Standard deviations were measured. Any data that contained crack length-to-width ratios (a/w) outside the 0.3 to 0.7 limits were not used in the data reduction procedure.

Flexural modulus measurements

Specimen and test fixture details. The American Society for Testing and Materials Specification (ASTM E966) was followed for measuring the flexural modulus of the bismaleimide networks. Samples were cast in silicone rubber moulds, as previously described, to obtain specimens of dimensions 1.5 mm × 13 mm × 52 mm. Testing was performed in a three-point bend apparatus and took place at a constant crosshead displacement of 1 mm min^{-1} until failure.

Data reduction. The following equation was used to calculate the flexural modulus E_B, given the specimen dimensions, chart speed, crosshead displacement and load at failure:

$$E_B=\frac{L^3M}{4bd^3}$$

where b = width, d = thickness, M = slope from stress–strain plot and L = span length (63 mm).

Scanning electron microscopy

Morphologies obtained within the neat resin, when thermoplastic modifiers phase separated from the thermosetting networks, were studied from fracture surfaces using scanning electron microscopy (SEM). This technique also enabled composite fracture surfaces to be studied, as well as polished composite laminate cross-sections, where morphology translations from neat resins to carbon-fibre composites were observed. All SEM micrographs were performed using an International Scientific model S X-40 apparatus using conductive silver paint as a mounting adhesive. Fracture surfaces were mounted on aluminium substrates and coated with approximately 100 Å of gold using a Bio-rad Polaron (model E5400) high-resolution sputter coater. Typically, electron beam voltages of 10 000 V were used; however, this was sometimes increased to 15 000 V if focusing was desired at higher magnifications.

Energy-dispersive spectroscopy

A useful attachment on any scanning electron microscope is an energy-dispersive spectrometer (e.d.s.). Back-scattered X-rays that occur from the surface bombardment by incident electrons are gathered, and their energies analysed. Each energy is specific to the element from which it came, thus allowing a fracture surface SEM to be mapped in terms of individual elements. Since sulphur was present in the polysulphone backbone, but not in the two thermosetting monomers, sulphur mapping using e.d.s. indicated the relative abundance and location of thermoplastic modifier within a fracture surface. To prevent sulphur peaks from being masked by large peaks from gold, fracture surfaces were sputtered with silver using the Bio-rad Polaron (model E5400) when any e.d.s. monitoring was required. Each surface micrograph was scanned 128 times, forming a resolution mapping diagram containing 128 × 128 pixels.

RESULTS AND DISCUSSION

Varying-toughness-backbone chemistry and the effect on viscoelastic properties

Figure 3 illustrates the chemical composition for various amorphous functionalized engineering thermoplastics used in this study. As one passes from

top to bottom in the figure, polymer backbones become more rigid and the glass transition temperature increases. Bismaleimides have upper service temperatures of approximately 230°C[7] for certain short-service-time applications, while other aerospace applications (leading edges on aircraft wings) may have upper service temperatures in the range 150–200°C. An important parameter to monitor when modifying thermoset networks is storage modulus retention at temperature values approaching the upper service limits. Dynamic mechanical thermal analysis is an excellent tool for such measurements. *Figure 5* depicts the retention in storage modulus as a function of temperature for three modified networks. All samples were cured for 1 h at 200°C and 2 h at 250°C, then slowly cooled at 3°C min^{-1} to room temperature. These samples varied in the modifier's chemical composition, which was found to alter the modifier's T_g. Other parameters such as modifier molecular weight (10 000 g mol^{-1}), end-group functionality (maleimide-terminated) and weight per cent incorporation (20% by weight) were all kept constant. The d.m.t.a. results clearly illustrate that the modifier's glass transition temperature controls the onset of decline in storage modulus. Therefore, a modifier's glass transition temperature must be considered when designing a thermoset network to meet specific applications. An example could possibly be related to creep phenomena, not usually encountered with highly crosslinked thermoset resins, which might produce problems with thermoplastic-modified networks.

Effect of varying the modifier's backbone structure on fracture toughness values

Table 1 details the fracture toughness properties for three amorphous thermoplastic modifiers with different backbone structures. The number-average molecular weight for each modifier was theoretically 10 000 g mol^{-1}. The table lists the amine precursor titration (prior to end-capping modifiers with maleic anhydride) for molecular weight as well as the intrinsic viscosities and glass transition temperatures for the three amorphous polymers. Fracture toughness measurements were made at both 10 and 20% by weight incorporations. The K_{Ic} values decreased with increasing modifier rigidity, as reflected by higher glass transition temperatures, thus suggesting that the thermoplastics' inherent ability to deform plays a major role in the fracture toughness properties of modified BMI networks. This appears reasonable if one considers that a similar network toughened with 10% by weight carboxyl-terminated butadiene–styrene rubber would yield higher K_{Ic} values (approaching 2–3 MPa $m^{1/2}$, for example). Although this trend seems feasible, conclusive statements concerning the polymer rigidity are difficult to make owing to the error involved in K_{Ic} determinations.

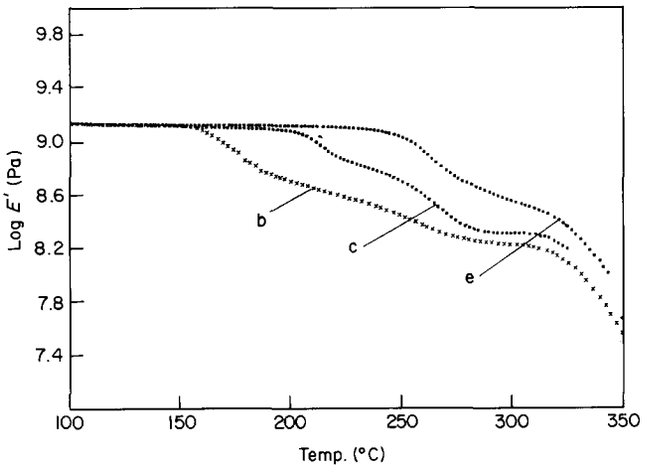

Figure 5 Storage modulus against temperature for modified networks containing thermoplastic polymers with various backbone structures; 20 wt% thermoplastic modifier in BMI–DABA. The curves b, c and e correspond to the modifiers in *Figure 3*

Having varied the modifier parameters of molecular weight, backbone structure and end-group functionalities, a comparison was made between the morphologies produced by two polymers that differed only by a subtle backbone modification. These polymers included a polysulphone synthesized using bisphenol A monomer and a polysulphone synthesized using tetramethyl bisphenol A. *Figure 3* illustrates the differences between the two polymer structures. *Figure 6* illustrates morphologies resulting from a 20% by weight incorporation of polymer with molecular weight held constant at 10 000 g mol^{-1}, and both having amine end-group functionalities. By introducing the tetramethyl bisphenol A moiety into the backbone structure, a morphology was created where both thermoset and thermoplastic were co-continuous. Interestingly, the fracture toughness of the network containing tetramethyl-based polysulphone was 0.9 MPa $m^{1/2}$ compared with 1.1 MPa $m^{1/2}$ for the bis-A polysulphone. Explanations for this difference may be attributed to the phase-inverted morphology being favourable for improved fracture toughness with more interfacial surface area being present in the phase-inverted case. A second explanation could be that the tetramethyl bis-A polysulphone was a less ductile polymer, owing to restricted bond rotation around the phenyl rings where the tetramethyl groups reside.

Molecular-weight effect of the toughness modifier

Table 2 lists the K_{Ic} fracture toughness values for amine-terminated polysulphone modifiers that vary in theoretical molecular weights from 5000 to 15 000 g mol^{-1}. Their intrinsic viscosities, glass transition temperatures and number-average molecular weights are also reported. Each property, including the fracture toughness value, increased with the modifier's increasing molecular weight

Table 1 Fracture toughness values for various polymer modifiers possessing different backbone structures

Polymer backbone	M_n (g mol^{-1}) Theory	M_n (g mol^{-1}) Precursor titration	$[\eta]$, $CHCl_3$, 25°C (dl g^{-1})	T_g (°C)	K_{Ic} (MPa $m^{1/2}$) 10 wt%	K_{Ic} (MPa $m^{1/2}$) 20 wt%
Polysulphone	10 000	12 800	0.25	186	1.0±0.2	1.4±0.3
Poly(ether phosphine oxide)	10 000	11 400	0.23	226	0.9±0.2	–
Polyimide	10 000	10 200	0.32	284	0.8±0.3	1.3±0.3

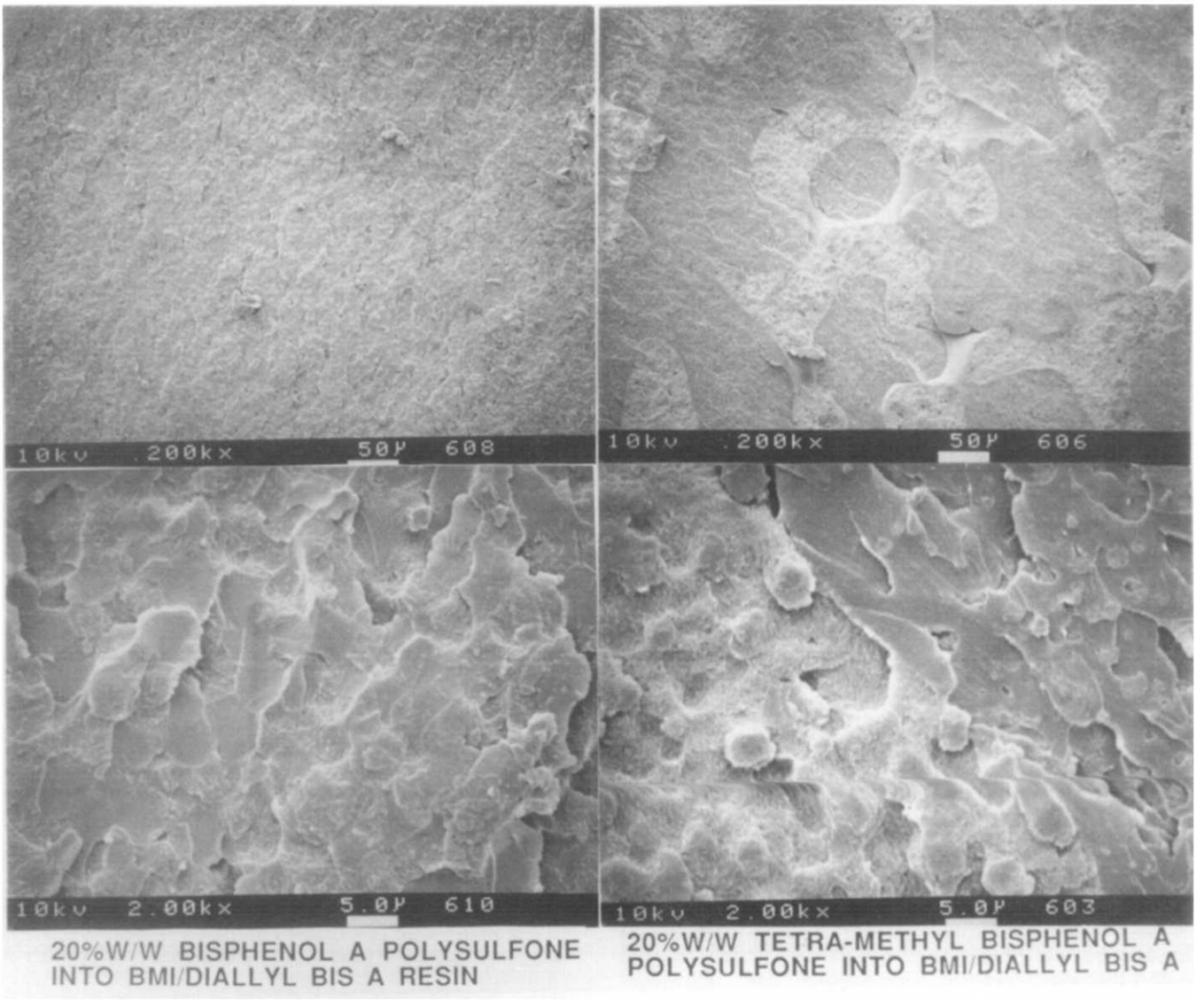

Figure 6 SEM micrographs illustrating the difference in morphology obtained by changing only the backbone structure in poly(arylene ether sulphone). Subtle changes in modifier backbone produce large changes in blend morphologies

Table 2 Fracture toughness values for amine-terminated polysulphone modifiers that vary in their molecular weight

M_n (g mol^{-1})		$[\eta]$, 25°C, $CHCl_3$		
Theory	Titration	(dl g^{-1})	T_g (°C)	K_{Ic} (MPa m$^{1/2}$)
5000	6000	0.13	166	1.0±0.2
10000	10900	0.18	178	1.1±0.2
10000	12800	0.22	182	1.4±0.2
15000	15760	0.27	181	1.5±0.1

(the weight per cent incorporation was maintained constant at 20 wt%). As described in the following section, all of these modifiers exhibited a phase-inverted morphology. The only work published concerning possible failure mechanisms for this morphology was reported by Brown and Kim[8]. Their optical observations on the failure mode of thin films possessing phase-inverted morphologies showed the existence of both interfacial failure and plastic deformation in both phases. The thermoplastic continuous phase exhibited ductile failure behaviour within the fracture process. The increase in fracture toughness with increase in modifier molecular weight tends to support these findings. The effect of modifier molecular weight on fracture toughness is illustrated in *Figure 7*. Such evidence supports the theory that one factor affecting fracture toughness in these modified networks is the inherent ductility of the modifier.

The fracture surface of the phase-inverted BMI resins exhibited cleaved thermoset spheres (see *Figure 8*). These features were not observed before with the modified epoxies. These facts suggest that, with good interfacial bonding between the phase-separated domains, the thermoset spheres are the limiting phase during the BMI fracture process. Such an observation leads one to propose that, for further improvement in the fracture toughness of these modified BMI systems, the thermoset spheres need to respond in a more ductile fashion. A higher incorporation of more phase-mixed species may be one solution, and should be the subject for future investigations.

Examining the fracture surfaces from each specimen revealed that molecular-weight changes associated with the toughness modifiers did not affect the resultant morphologies (*Figure 8*). The morphology is termed 'phase-inverted' since the thermoset monomers that form

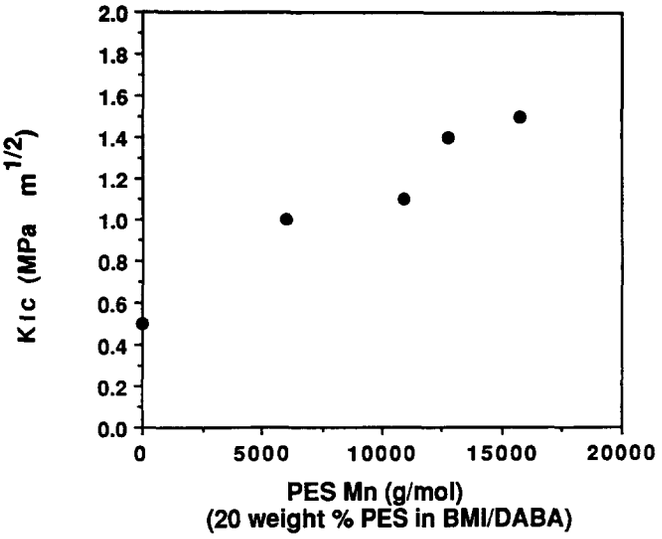

Figure 7 Critical stress intensity as a function of modifier molecular weight

the crosslinked phase form the larger volume fraction, yet become discrete spheres surrounded by a continuous phase of thermoplastic. Upon closer examination, a coating surrounding the spheres was apparent. This coating was the polysulphone, and excellent adhesion between the thermoplastic and thermoset phases occurred due to the reactive end-groups present on the polysulphone modifier.

In certain regions, the micrographs illustrate how some spheres appear to have been cleaved in the fracture process and a smooth grey surface remains. E.d.s. was a valuable analytical tool for probing these phase-separated morphologies. *Figure 9* compares an e.d.s. sulphur map with the corresponding fracture surface from which it was developed. Sulphur atoms are present in the polysulphone modifier, but not in the thermoset monomers. The relative abundance of modifier within a surface micrograph can therefore be estimated. White areas represent high-intensity sulphur regions, whereas black areas are regions of low intensity. The e.d.s. map depicts white areas around dark circular regions (which correspond to cleaved spheres) and were experimental evidence of the phase-inverted morphology. On the e.d.s. map, a good example can be seen in the five dark circular regions located top-centre. These correspond to the five fractured spheres in the same position on the surface micrograph. The presence of a third species representing a thermoplastic–thermoset alloy was evident from a third peak present in the three-dimensional loss tangent (E''/E'), temperature and weight per cent modifier plot (*Figure 10*). This third peak is located between the pure thermoset and thermoplastic glass transitions, and steadily increases in intensity as the polysulphone weight per cent loading was increased.

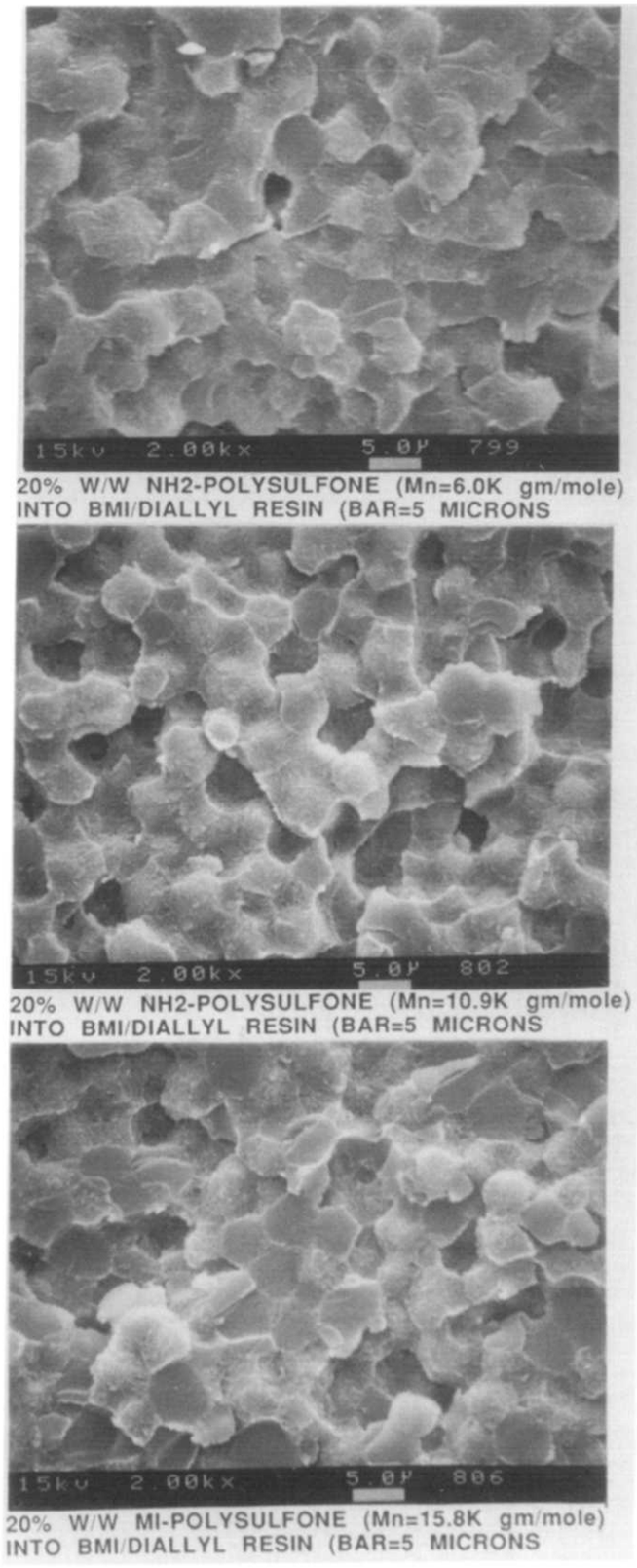

Figure 8 Molecular weight of the toughness modifier does not alter the fracture surface morphologies at 20 wt% incorporation

Effect of amount of toughness modifier incorporated

Table 3 presents K_{Ic} fracture toughness results for various weight per cent loadings of poly(ether sulphone) and polyimide modifiers. For each polymer, increasing the modifier content resulted in an increase in the K_{Ic} fracture toughness values above the 0.5 MPa $m^{1/2}$ obtained for the control. Maximum weight per cent loadings approached 25–30%. This value depended upon the modifiers' molecular weights. The highest molecular weights in combination with high weight per cent loadings resulted in high viscosities when preparing the homogeneous hot-melt solutions, thus making sample preparation for various specimens increasingly difficult.

Approximately three-fold increases in fracture toughness values were measured at weight per cent incorporations

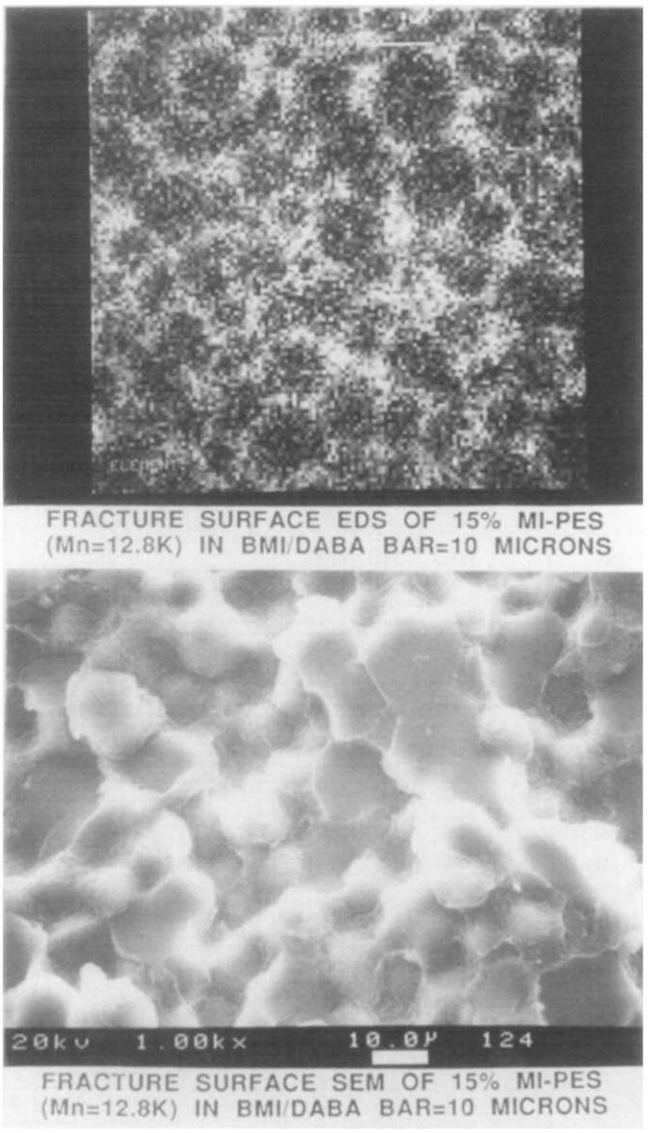

Figure 9 Sulphur mapping using energy-dispersive spectroscopy to probe the interior of a fractured phase-inverted sphere

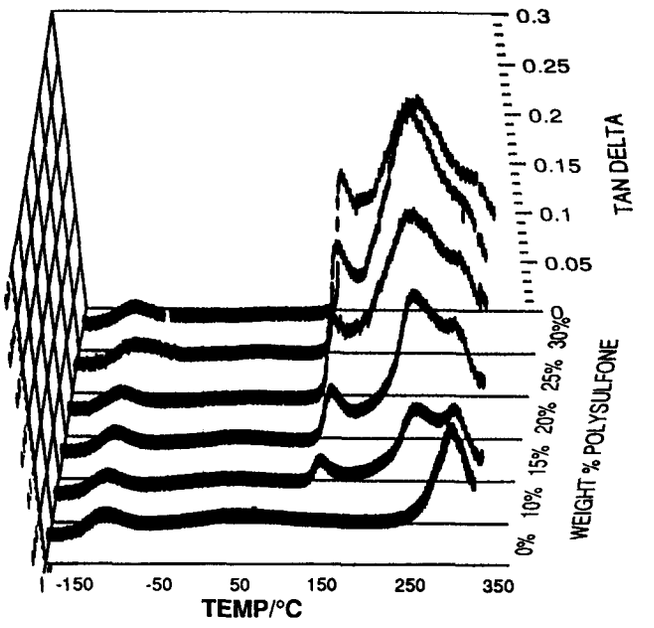

Figure 10 Three-dimensional plot of tan δ, temperature and weight per cent incorporation illustrating the presence of a third species representing a thermoplastic–thermoset alloy

Table 3 Fracture toughness values K_{Ic} (MPa $m^{1/2}$) for various weight per cent loadings of polysulphone and polyimide modifiers

MI–PES incorporation (wt%)	MI–polyimide	
	$M_n = 12\,800$ g mol^{-1}	$M_n = 10\,200$ g mol^{-1}
0	0.5±0.2	0.5±0.2
10	1.0±0.2	0.8±0.3
15	1.2±0.2	–
20	1.4±0.3	1.3±0.3
25	1.5±0.2	–
30	–	–

of 20% and higher. This is confirmed by analysing the fracture toughness column in *Table 3* for the maleimide-terminated polysulphone modifier with $M_n = 12\,800$ g mol^{-1}. Values tended to increase and then level off with increases in weight per cent loadings, unlike those reported by Recker and coworkers[2], who observed that the toughness values went through a maximum.

When commercial engineering thermoplastics were used to modify the BMI resin, gross phase separation occurred. *Macroscopic* phase separations typically lead to low fracture toughness values; thus, phase separation on a *microscopic* level, 0.1–5 μm, was desired. A major problem with employing commercially available engineering thermoplastics is that they were not specifically designed for use as reactive modifiers. Their end-groups are typically unreactive (to ease in processing when injection moulding, for example). All molecular weights are high to ensure good mechanical integrity, but limiting use to low weight per cent incorporations into hot-melt resins. By lowering molecular weights, higher weight per cent loadings into hot-melt processable resins may be achieved, and as a result provide a spectrum of morphologies. *Figure 11* illustrates the variations in morphology as one increases the weight per cent loading for polysulphone modifier from 10% through to 25%. At 15, 20 and 25% the phase-inverted morphology is observed, which densifies as the thermoplastic content increases. At 10% loadings, a mixed morphology was present, where both continuous thermoset and thermoplastic phases existed simultaneously. At low loadings, continuous thermoset surrounded thermoplastic nodules.

Effect of various toughness modifier end-groups

A procedure is presented in *Figure 4* for preparing oligomers of various end-groups starting from amine-terminated oligomers. This method was utilized to prepare large quantities of polysulphone modifier that varied only in end-group chemistry, i.e. amine, maleimide and phthalimide. Amine-terminated polymers can react with the growing BMI–DABA network via a Michael addition reaction. The maleimide functionality has several possible mechanisms for reacting with the growing network[9]; however, polysulphone modifiers with phthalimide end-groups are not expected to react with the thermosetting monomers. The K_{Ic} fracture toughness results produced by changing only the end-group type are summarized in *Table 4*. Polymer backbone structure, molecular weight and per cent of toughener incorporation were all kept constant. The unreactive phthalimide

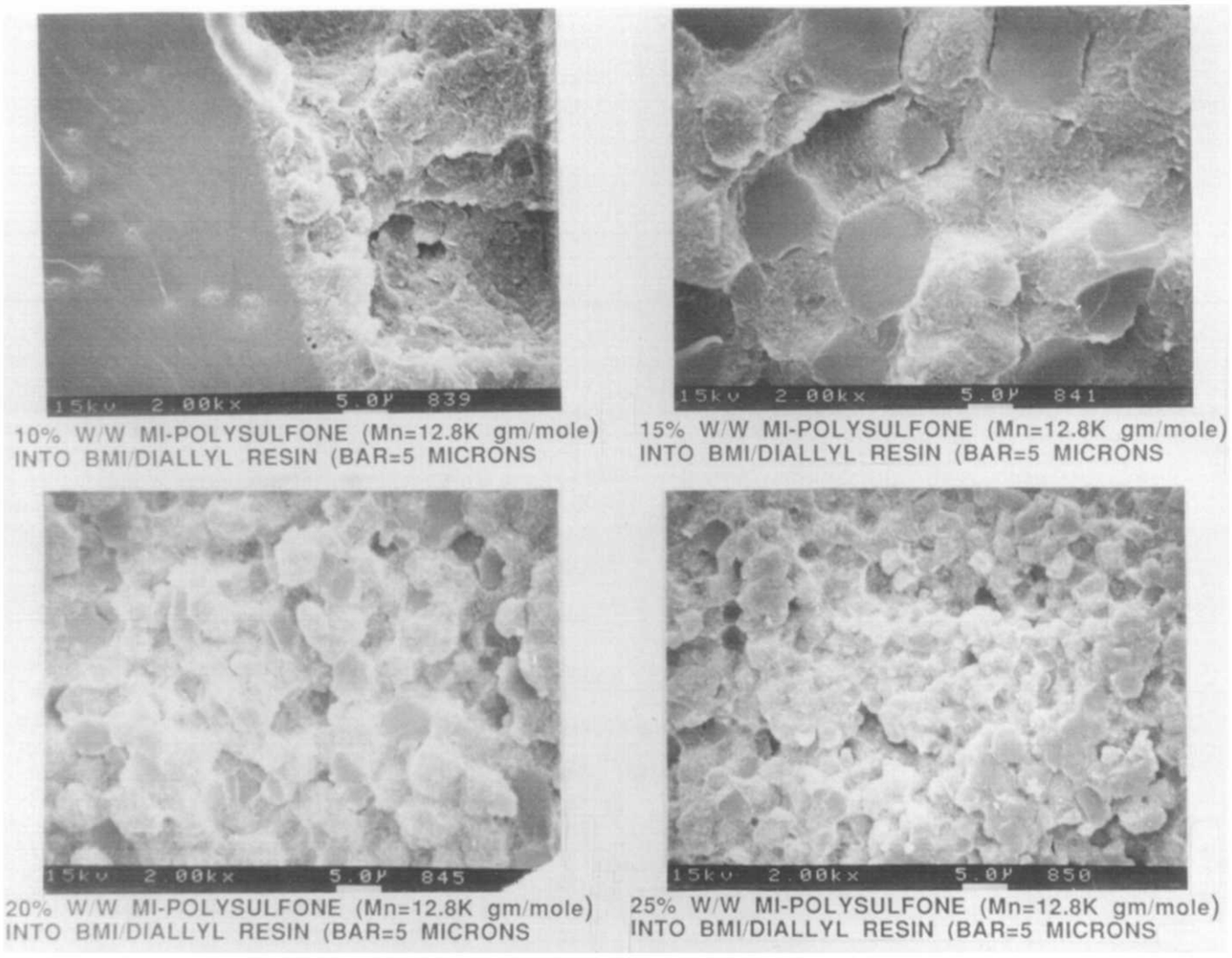

Figure 11 SEM micrographs of fracture surfaces illustrating the effect on morphology of varying the weight per cent incorporation from 10 to 25 wt% of the polysulphone modifiers into the thermoset network

Table 4 Fracture toughness variations by changing only the end-group functionality on polysulphone modifiers

End-group	K_{Ic} (MPa m$^{1/2}$)	T_g (°C)	$[\eta]$, 25°C, $CHCl_3$ (dl g^{-1})
Phthalimide	0.9±0.2	182	0.25
Amine	1.4±0.2	182	0.22
Maleimide	1.4±0.3	186	0.25

end-groups should not provide good adhesion between the phase-separated thermoplastic and the thermoset phases. This is in contrast to the amine and maleimide functionalities, which are expected to provide excellent adhesion. This improvement in adhesion was reflected in the improved fracture toughness values when amine and maleimide functional polymers were utilized, as compared with the unreactive phthalimide end-capped modifier.

Scanning electron micrographs illustrating the fracture surfaces from specimens detailed in *Table 4* are given in *Figure 12*. With the constant loading of 20 wt%, each micrograph exhibits the phase-inverted morphology. Fracture surfaces from modified networks containing amine- and maleimide-terminated polysulphone modifiers were very similar. As described previously in these two cases, cleaved thermoset spheres were evident. In contrast, on inspecting the micrograph illustrating the fracture surface from a network modified with phthalimide end-capped polysulphone, it was apparent that no thermoset spheres had been cleaved. The later micrograph depicts whole spheres coated with a continuous phase, and suggests that the fracture process had caused a separation or pull-out effect. From the fracture toughness values and their corresponding fracture surface micrographs, it seems quite possible that a change in failure mechanisms occurred due to the difference in adhesion levels at the interface between the phase-separated domains.

Resistance to hydroxide ions

Quite recently, concern has been expressed in the composites industry following an announcement by General Dynamics[10] that certain carbon-fibre composites containing polyimide resins were being degraded by a galvanic corrosion process. A small symposium at SAMPE 91 was dedicated to discussing this problem[11]. Although the whole degradation process is not clearly understood, an electrochemical cell was apparently set up at the interface between carbon fibres and imide resins when the composite material was immersed in a metal

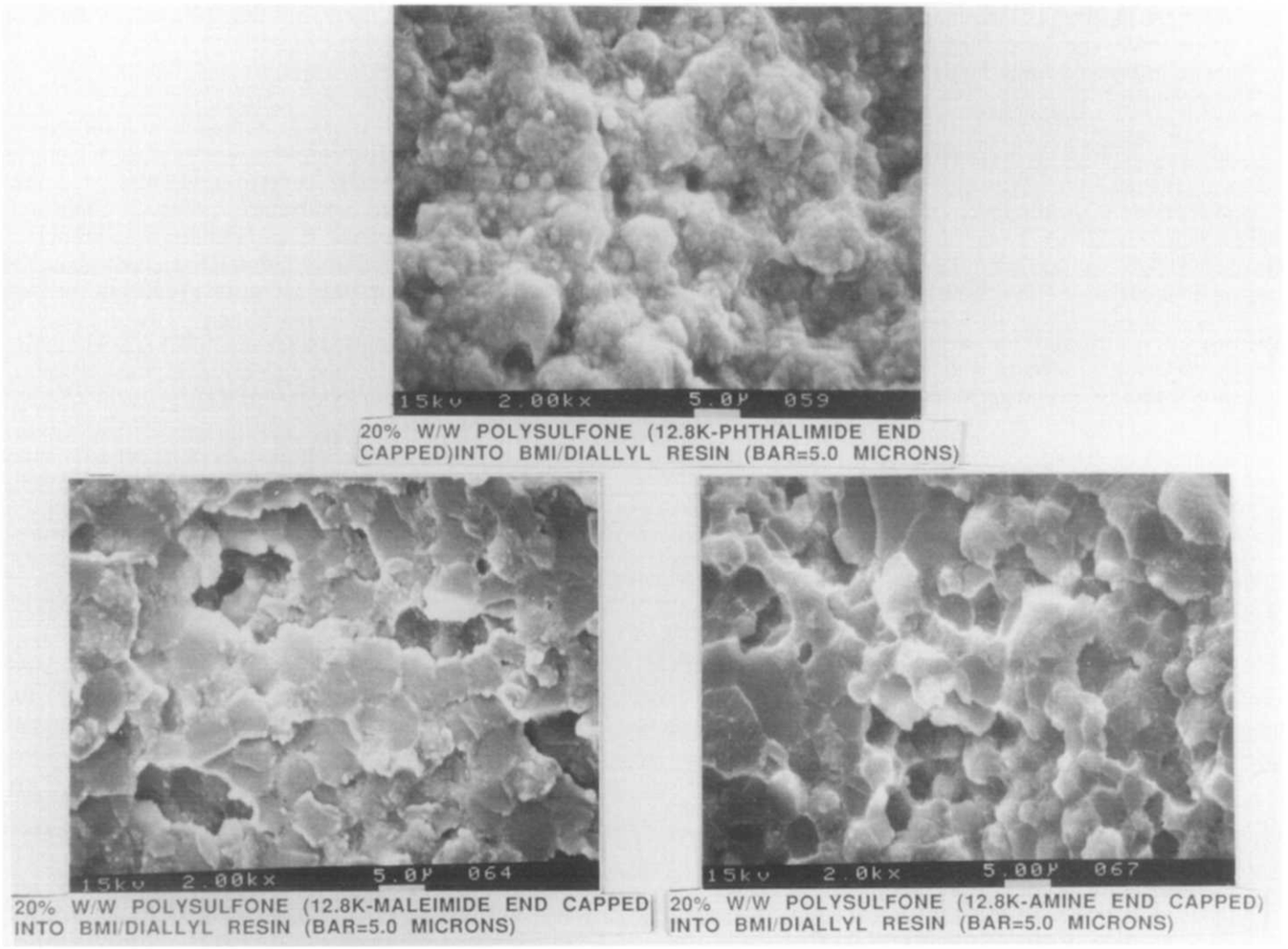

Figure 12 Fracture surface micrographs for modifiers varying only in their end-group functionality

(tin) vessel containing salt water. The electrochemical reaction appears to be forming a high hydroxide ion concentration within the composite laminates, which was possibly causing the imide ring to open, leading to degraded composite properties. The problem could be extremely hazardous when uses for polyimide composites are being sought in naval applications, where the composite parts are joined together using metal fasteners. Protective coatings on laminate parts may not be sufficient to stop the electrochemical attack. However, a protective coating within the matrix material could inhibit the property degradation. A continuous polysulphone phase (which is resistant to hydroxide attack) surrounding the imide material (i.e. the phase-inverted morphology) could provide a solution to this problem. To examine this possibility, some flexural modulus specimen bars were immersed in concentrated potassium hydroxide solutions (40%), and periodically removed for 90° flexural modulus measurements. Two specimen types were chosen. One was a control BMI containing no polysulphone modifier, while the other contained 20% by weight of polysulphone, and thus exhibited the phase-inverted morphology within its network. The mean values from five specimens of each type are presented in *Figure 13*. These data clearly illustrate how the polysulphone coating protected the modified network from any decrease in modulus. In contrast, a steady

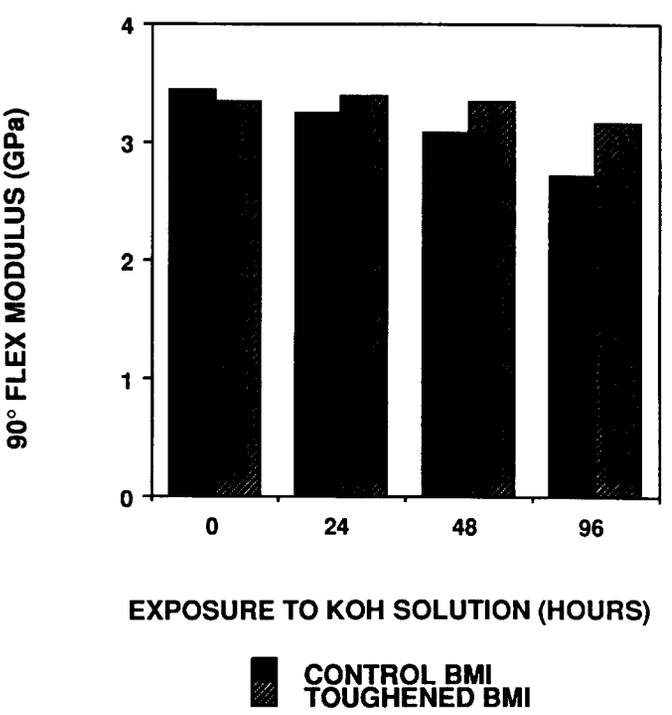

Figure 13 Phase-inverted morphology protects BMI from attack by hydroxide ions

reduction in flexural modulus was apparent for the control BMI specimen, suggesting that the hydroxide ions had attacked some imide groups, thereby lowering the modulus.

COMPOSITES

COMPOSITE PROCESSING

Materials

Unidirectional carbon-fibre prepreg tape was prepared using Hercules IM7 unsized, 12K, carbon fibre. The hot-melt resin solutions were prepared as previously described and added to a heated resin bath within a drum winding prepregging machine. Essentially, the prepregging process consists of a single carbon-fibre tow unwinding from a tension-controlled spool. It passes over a series of guide rollers and drops vertically to enter the resin pot. After passing over flattening pins located inside the resin, the fibre tow exits a wedge slit die located directly beneath the pot. The tow travels down and around a guide roller (heating optional) that contains a groove of specific dimensions for the fibre type (i.e. AS4 or IM7 for example). The drum is controlled in terms of its revolutions per minute and traverse speed. The process is depicted schematically in *Figure 14*.

Laminate cure cycle

All the neat resin specimens were cured for 1 h at 200°C and 2 h at 250°C with a 3°C min^{-1} slow cool to room temperature. The cure cycle for the unidirectional laminates was similar to that used for the neat resin specimens. However, for the laminates, pressure was applied after a dwell period of 30 min at 130°C. A vacuum bag containing prepreg lay-up was located within the press between the platens and centred to ensure that even pressure was applied to the entire laminate specimen. The platens were closed to subject the mould to only contact pressure, and heated at 5°C min^{-1} to 130°C. Upon reaching 130°C an isothermal hold was maintained for 30 min, after which the temperature was raised to 200°C at a 3°C min^{-1} heating rate. During this temperature ramp the pressure was increased 50 psi (~345 kPa) at 5 min intervals until the pressure reached 200 psi (~1380 kPa). The laminates were held at 200°C under 200 psi pressure for 1 h, after which the power to the platens was turned off, but pressure maintained as the mould slowly cooled to room temperature. Prior to mechanical testing, each laminate was C-scanned to check for voids.

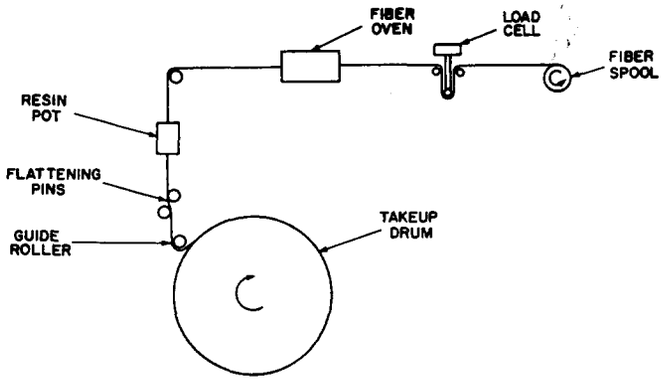

Figure 14 Schematic diagram of the drum winding prepregging process

Mode I and mode II testing for composite strain energy release rates

The mode I strain energy release rate G_{Ic}, a measure of the composite material's fracture toughness, was measured using a double cantilever beam specimen geometry. Test coupons were machined using a diamond saw (cooled with water) from 152 mm × 152 mm (6 inch × 6 inch) unidirectional panels specifically laminated to produce G_{Ic} specimens. Each laminate was prepared from 18 plies of carbon-fibre prepreg to make laminates approximately 2.5 mm (0.10 inch) thick. During the ply lay-up a 152.4 mm × 50.8 mm (6 inch × 2 inch) piece of Kapton® film was inserted after nine plies (the laminate mid-thickness point) at one end of the lay-up to act as the crack initiator (or defect starter). The protocol[12] being followed for G_{Ic} testing suggested the starter film length should be greater than 50 mm (1.97 inch), so that any influences from the hinges could be neglected. Typical specimen dimensions were 152.4 mm (6 inch) in length, 12.7 mm (0.5 inch) wide and nominally 2.5–3.5 mm thick.

Brass piano stock hinges were adhered to the specimen ends using cyanoacrylate adhesive and primer after carefully preparing and cleaning the adherend surfaces (both composite and hinges) with sandpaper and subsequent rinses with water and acetone. Care was taken to ensure that both hinges on each specimen were in alignment since the direction of applied load for the mode I crack opening within the specimen would be dictated by this alignment. The hinges must be free to rotate so that minimal stiffening of the G_{Ic} specimen is introduced when attached to the Instron grips. The protocol followed for measuring G_{Ic} values suggested that specimens should not be precracked. That is, the initial crack must be started at the starter defect ends upon continuous load displacement at the initial stages of the G_{Ic} measurement. However, the double cantilever beam was pre-opened (without initiating the starter crack) to prevent large crack running at the initiation point. This was done by placing the specimen in vice grips where the Kapton film end was held firmly together. At the same time a razor blade was utilized to open the displacement between the two specimen halves, and was pushed vertically down into the specimen along the Kapton film surface to a distance of approximately 44.5 mm (1.75 inch).

Test procedure. The load read-out at zero displacement was minimized by careful alignment of the grips as the specimen was attached. Twisting could easily be introduced at this stage and could create erroneous load readings. Great care was taken to minimize twisting and the specimen was loaded using a crosshead rate of 0.5 mm min^{-1} (0.02 inch min^{-1}). This rate was chosen to allow crack propagation to be followed and recorded easily. Crack propagation was monitored using a large magnifying glass situated in front of the specimen. Digital calipers were used to monitor the crack length, the end of which could be visually observed. A smooth coating of liquid paper was applied to the specimen edge to aid in the crack length measurements. Approximately 45–50 crack length values were obtained, including the corresponding displacement value (d) and the load being carried by the double cantilever beam (P).

Data reduction. The Berry data reduction approach was followed to obtain G_{Ic} values[12]. This scheme uses the experimental compliance calibration method.

Numerous methods exist to reduce the data to yield the G_{Ic} values, and their relative merits are discussed in the literature[13,14]. Equation (2) describes the approximate relationship between the compliance C of the double cantilevered beam and the measured crack length a, where K and n are empirical parameters:

$$C = Ka^n \tag{2}$$

Ward[15] has described the advantages of using this method, which by-passes the question regarding plane stress or plane strain deformation. The value of n can be obtained by plotting log C against log a, and finding the slope as:

$$\log C = \log K + n \log a \tag{3}$$

The value determined for n is substituted into equation (4) to yield the strain energy release rate value as a function of the measured crack length, where B is the specimen width and P is the load being carried by the double cantilevered beam at the corresponding crosshead displacement d:

$$G_{Ic} = \frac{nPd}{2Ba} \tag{4}$$

In a plot of G_{Ic} as a function of crack length a, the plateau region is taken to be the constant strain energy release rate and by extrapolating to the y axis one obtains the desired G_{Ic} value.

G_{IIc} *fracture toughness*

Specimen and test fixture details. The mode II strain energy release rate G_{IIc}, a measure of the composite material's fracture toughness when a crack is being opened through shear, was studied using an end-notched flexure specimen developed by Russell and Street[16]. Test coupons were machined in the exact manner as described for the mode I test coupons and the crack pre-opened, but not precracked, in a similar fashion. The specimens were cut from the same 152.4 mm × 152.4 mm (6 inch × 6 inch) unidirectional panels as the G_{Ic} specimens that contained the Kapton film inserted at the laminate mid-point. Typical specimen dimensions were again 152.4 mm (6 inch) in length, 12.7 mm (0.5 inch) wide and approximately 2.54 mm (0.10 inch) thick. The Instron testing machine (model 4204) was fitted with a three-point bend apparatus and run in compression. A fixed span length of 100 mm was used.

Test procedure. Samples were initially loaded without the starter crack being inside the span length. A stress–strain response was obtained from which a compliance value for the beam without the Kapton film was calculated. After obtaining the elastic response, the specimen was turned around and loaded within the three-point bend apparatus so that the crack length a equalled 25 mm. This would ensure that the a/L ratio was 0.5. The width and thickness for each specimen were measured at the specimen centre and at either end; average values were recorded. The specimen was loaded in compression at a rate of 0.5 mm min^{-1} (0.02 inch min^{-1}). A load–displacement plot was recorded: as the specimen was loaded, the crack propagated to the centre, and the load dropped sharply. Typically, the stress–strain plot would become non-linear, reach a maximum value and decrease. The data treatment for both the non-linear and maximum load points are given in the following section.

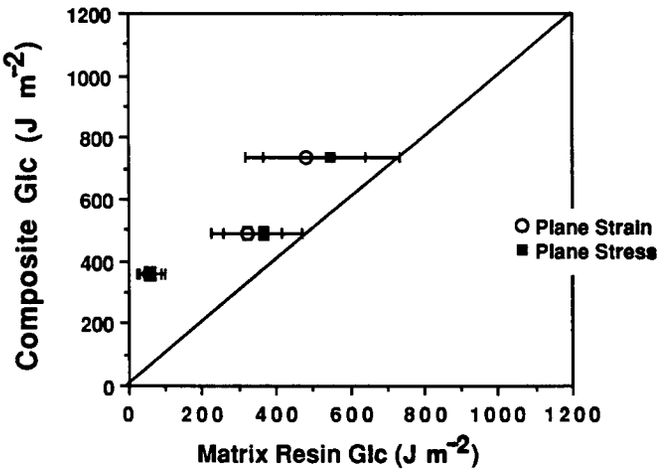

Figure 15 Composite strain energy release rate plotted against matrix strain energy release rate

Data reduction. Several G_{IIc} values may be determined from the experiment. The two described here are the G_{IIc} values calculated from the non-linear point G_{IIc}(nl) and G_{IIc}(max), where the maximum load and the corresponding displacement point are used. A schematic diagram for a typical load–displacement plot is illustrated in *Figure 15*. The following calculations were used:

$$G_{IIc} = \frac{9a^2P_{nl}^2C_{nl}}{2B(2L^3 + 3a^3)} \tag{5}$$

where P_{nl} = load at non-linear point, B = specimen width, L = half span length (50 mm), a = crack length, C_{nl} = calculated compliance using experimental compliance calibration and h = specimen thickness, with

$$C_{nl} = \frac{2L^3 + 3a^3}{8E_{a=0}Bh^3} \tag{6}$$

and

$$E_{a=0} = \frac{L^3}{4BC_ih} \tag{7}$$

The value of C_i in equation (7) was taken from the initial plot where stress–strain was measured with no crack length placed between the spans. $E_{a=0}$ was calculated and substituted into equation (6). The calculated compliance C_{nl} was substituted into expression (5) for the G_{IIc}(nl) determination.

In some cases, the load–displacement curve changed from linear to non-linear as the initial crack length a was changed slightly during the non-linear portion. A new value for the crack length, a_{equiv}, needed to be calculated, and equations (8) and (9) detail the necessary calculations to evaluate G_{IIc}(max):

$$G_{IIc}(\max) = \frac{9a_1^2P_{max}C_{max}}{2B(2L^3 + 3a_{equiv}^3)} \tag{8}$$

$$a_{equiv} = \frac{C_{max}8E_{a=0}Bh^3 - 2L^3}{3} \tag{9}$$

where $E_{a=0}$ is calculated using equation (7) and C_{max} was calculated from the compliance corresponding to the maximum load[17].

RESULTS AND DISCUSSION

Composite fracture toughness values

Table 5 describes the mode I strain energy release rate values (G_{Ic}) measured using a double cantilevered beam specimen for unidirectional carbon-fibre laminates that contain 0, 15 and 20 wt% loadings of a maleimide-terminated polysulphone toughness modifier (M_n = 12 800 g mol^{-1}). The table illustrates how the composite G_{Ic} values increased with increasing polysulphone content to a respectable value of 743 ± 10 J m^{-2} for the 20% toughened resin (359 ± 17 J m^{-2} for the control). The stress intensity factors (K_{Ic}) for the neat resin samples were measured. By knowing the modulus of these specimens, the strain energy release rate values (both plane stress and plane strain) were calculated for the neat resin samples and are listed in *Table 6* and plotted in *Figure 15*, in a similar manner to the plots described by Hunston[18]. The error bars for the neat resin values are relatively wide since errors from K_{Ic} and flexural modulus measurements have been propagated. A 45° line has been drawn through the graph to illustrate a one:one fracture toughness relation. A clear observation is that the composite strain energy release rate values are higher than their neat resin counterparts. A possible explanation for this higher fracture toughness measurement could lie in the fibre bridging/nesting phenomena. Also, the fact that higher resin contents were observed in the 15 and 20 wt% systems (50% resin) may be important. Tough matrix resins are believed to possess high fracture energies due to the ability of these polymers to generate large crack-tip deformation zones and effectively blunt the crack tip[19]. Carbon fibres may restrict the growth of this deformation zone and produce composites with lower-than-expected fracture toughness values. A resin-rich laminate that has resin-rich regions, and therefore low fibre contents in the interlaminar zones, could create increased toughness translation by minimizing this fibre deformation zone restriction effect. Coupled with the fibre bridging phenomenon, another energy-absorbing mechanism, the composite material may reflect higher G_{Ic} values than the neat resin.

Fibre bridging and nesting occur when various plies do not remain in distinct layers but rather mesh (or nest) together with adjacent plies. Such an effect inhibits the crack propagation along a smooth plane; instead, the crack must move around the fibres, causing fibres to pull out and away from adjacent layers. This fibre pull-out phenomenon, which does create some fibre breakage, was observed with most of the unidirectional laminates prepared within this study.

Table 5 also describes the mode II results for these composite systems. The values increase with increasing polysulphone content but are extremely high, being above 2 kJ m^{-2}. Carbon fibre/PEEK (poly(ether ether ketone)) composites have been reported[20] to have values as high as 2.9 kJ m^{-2}. The excellent mode II toughness results for these modified BMI systems do tend to suggest that the resin-rich laminates have promoted high values, considering that crack opening in shear (mode II) would require large amounts of fracture energy in resin-rich zones. A crack opening typically occurs along the path of least resistance. In commercial fibre composites, an interlaminar crack may propagate within interply regions, since fibres from adjacent layers are typically close together. However, in laminates prepared in this study, a thin resin layer on the underside of the prepreg formed during the drum winding process. It is believed that this proceeded to form an *in situ* interlaminar toughening effect, and the propagating crack was forced to travel horizontally through the resin-rich interply areas. By restricting the crack's progression up into the interply areas, the high G_{IIc} values were obtained. A resin-rich zone in front of the crack tip could also be used to explain the high G_{IIc} values observed. Similarly, the fact that specimens were typically 3–3.5 mm thick and a thickness dependence has been observed for G_{IIc} values in carbon fibre/PEEK composites[21] might be important. Altstadt[22] has discussed this increase in mode II fracture toughness by describing the 'hackling' effect. Here it is believed that resin in front of the crack tip can open locally in mode I and then propagate in mode II. This vertical and then horizontal crack opening on a localized level in front of the crack tip can lead to jagged fracture surfaces that have been termed hackles. Restricting hackle formation can limit the interlaminar toughness. Conversely, allowing sufficient material within the interply region to form large hackles generates an energy dissipating mechanism that could lead to higher interlaminar fracture toughness values. Such explanations have been given as a driving force for developing special interlaminar toughening effects.

One approach to toughening is the introduction of interleaf systems[23,24]. These are based on a concept introduced commercially by American Cyanamid whereby a discrete layer of resin of very high toughness is added to a standard prepreg. By developing interleaf materials that co-cure with the matrix resin and remain as a discrete layer throughout the consolidation process, a composite material possessing superior compression after impact behaviour has been prepared[24].

Table 5 G_{Ic} and G_{IIc} values (J m^{-2})

	IM7/0% PES BMI/DABA		IM7/15% PES (12.8K–MI) BMI/DABA		IM7/20% PES (12.8K–MI) BMI/DABA	
Specimen	G_{Ic}	G_{IIc}	G_{Ic}	G_{IIc}	G_{Ic}	G_{IIc}
1	–	586	471	2589	739	2556
2	361	466	468	2576	719	2553
3	378	454	485	2564	733	2063
4	360	475	490	1673	746	2539
5	337	578	530	1875	–	2357
Mean	359	512	489	2255	734	2411
Standard deviation	17	65	25	399	10	189
Fibre volume fraction (%)	73	73	50	50	50	50

Table 6 Tabulated data for composite G_{Ic} against neat resin G_{Ic}

Polysulphone (wt%)	Flexural modulus (GPa)	Neat resin G_{Ic} (J m^{-2}) Plane stress	Neat resin G_{Ic} (J m^{-2}) Plane strain (n=0.35)	IM7 composite G_{Ic} (J m^{-2})
0	4.1 ± 0.8	60.8 ± 36	53.4 ± 31.7	359 ± 17
10	3.9 ± 0.7	366.0 ± 107	321.2 ± 94.0	489 ± 22
15	3.6 ± 0.5	549.0 ± 184	481 ± 161.0	734 ± 12

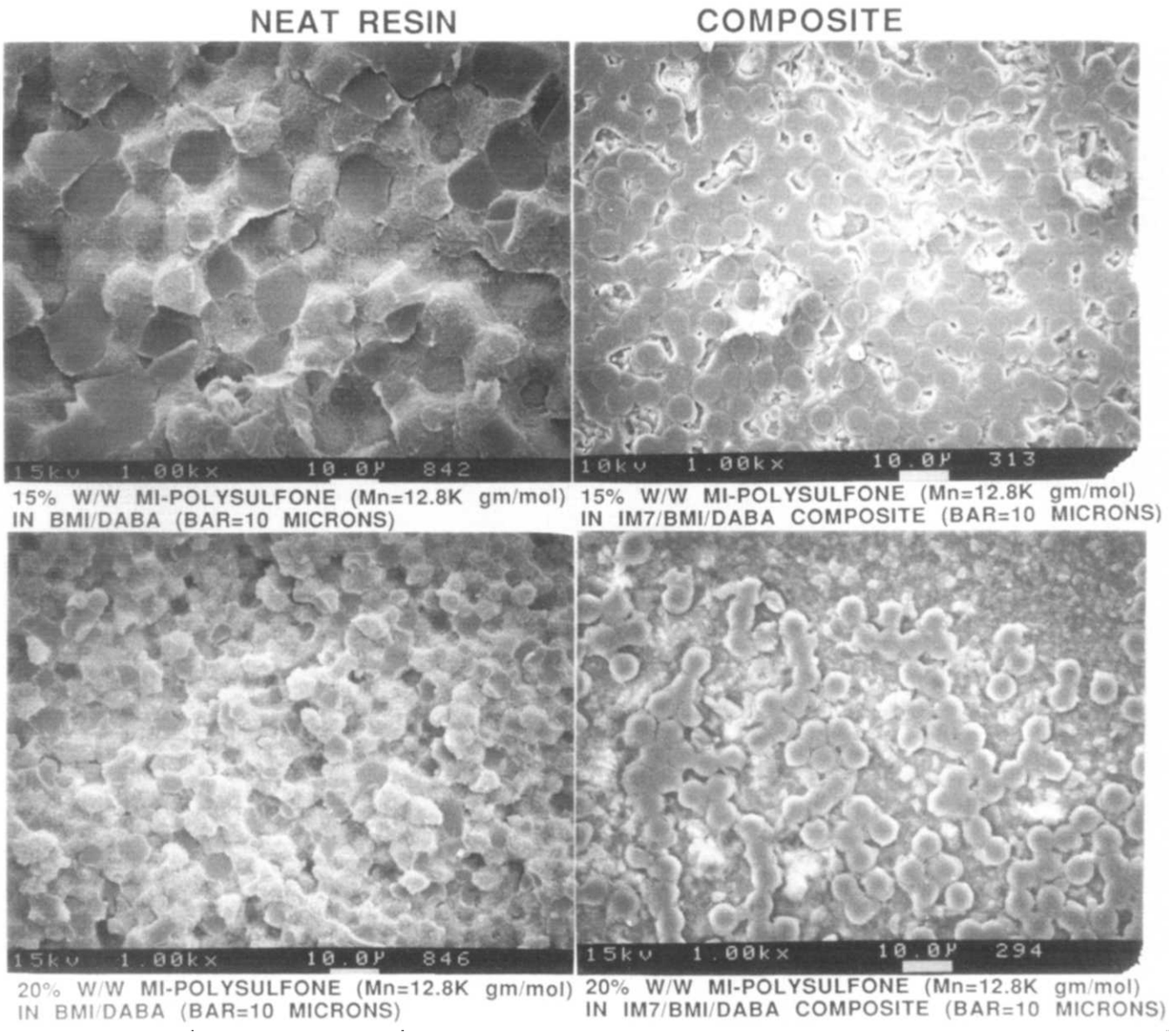

Figure 16 Morphology transfer from neat resin into the fibre composite: carbon fibres change morphology in composite material

One important feature of the presently reported materials that requires some attention is the neat resin morphological translation into the composite material. Polished cross-sections of the 15 and 20% polysulphone-toughened composites were subjected to a potassium permanganate/phosphoric acid etching process. After sonicating for 30 min the material was sputtered lightly with gold and the etched surfaces analysed on the SEM. *Figure 16* illustrates the neat resin morphologies in conjunction with their etched composite cross-sections. The large thermoset domains associated with the phase-inverted morphology are reduced in their dimensions. For example, the BMI modified with maleimide-terminated polysulphone (12 800 g mol^{-1}) illustrated in *Figure 16* (bottom left) has phase-inverted sphere dimensions of 7–8 μm in diameter. On the other hand an SEM micrograph on the bottom right of *Figure 16* illustrates, upon close inspection, that the phase-inverted morphology does exist within the laminate; however, the dimensions are much smaller, being of the order of 2 μm and less (top right-hand corner of the micrograph). The smaller domain size may also explain why higher G_{Ic} values were obtained in the composite compared to the neat resin. A denser formation of smaller phase-inverted spheres could provide an increase in the interfacial area between the phase-separated domains. This would result in more interfacial bonds being required to create fracture and hence would increase the fracture toughness. Such a hypothesis would have to be proved by future neat resin fracture toughness experiments if morphology could be controlled to create such differences in neat resin specimens, keeping all other parameters constant.

In summary, the high G_{IIc} values could be attributed to a combination of higher resin content, thick specimens, resin-rich areas within the interlaminar regions, and possibly to a dimensional change in the matrix morphology.

CONCLUSIONS

Significant improvements in fracture toughness of thermoplastic-modified BMI-based resins were achieved with ca. 20% by weight incorporation of a 12 000 g mol^{-1} toughness modifier. These oligomers toughen the thermoset matrix yet are low enough in molecular weight to maintain a low-viscosity hot-melt BMI solution, thus

enabling prepregging to be performed via conventional and commercially advantageous hot-melt techniques. Reactive end-groups contributed greatly to the improvements in fracture toughness by covalently linking the discrete and continuous phases. The resulting morphologies were observed to change as a function of both weight per cent loading and backbone structure. No particular morphology was noted from these studies for optimum fracture toughness. However, in the case where the phase-inverted morphology was observed, the adhesion of the thermoplastic-rich phase to the thermoset-rich spheres was noted to be an important factor in improving fracture toughness. For this specific morphology, such structure may be the key factor to control the failure mechanism within these thermoplastic–thermoset blends.

The mechanical test results for both mode I and mode II strain energy release rates illustrated excellent correlation toughness values of neat resin specimens to the composite materials. Respectable values of 489 ± 25 and $734 \pm 10\ J\ m^{-2}$ for the 15% and 20% polysulphone-toughened ($12\,800\ g\ mol^{-1}$) BMI networks were obtained from mode I tests. A resin-rich layer existed within the interlaminar region, as a result of the drum-wound prepreg, and was believed to contribute to the excellent translation of mode I properties. Also, this resin-rich zone was believed to be the cause of the high values obtained for the mode II tests. Interlaminar toughening appears to be an extremely effective method to toughen composite materials.

ACKNOWLEDGEMENTS

The authors would like to express their gratitude to the ICI Wilton Materials Research Centre and to the National Science Foundation Center for High Performance Polymeric Adhesives and Composites contract number DMR8809714 for supporting this research. Also, the help of Mr Jack Lesko during the mechanical testing of the composite laminates is gratefully acknowledged.

REFERENCES

1 Sefton, M. S., McGrail, P. T., Wilkinson, S. P., Peacock, J. A., Davies, M., Crick, P. and Almen, G. *Int. SAMPE Tech. Conf.* 1987, **19**, 700
2 Recker, H. G., Allspach, T., Altstadt, V., Folda, T., Heckmann, W., Itteman, P., Tesch, H. and Weber, T. *Int. SAMPE Tech. Conf.* 1989, **21**, 25
3 Johnson, R. N., Farnham, A. G., Clenndening, R. A., Hale, W. F. and Merriam, C. N. *J. Polym. Sci.* 1967, **5**, 2375
4 Maiti, S. and Mandal, B. K. *Prog. Polym. Sci.* 1986, **12**, 111
5 Segal, C. L. *Int. SAMPE Tech. Conf.* 1985, **17**, 147
6 Kwiatkowski, G. T., Robeson, L. M., Brode, G. L. and Bedwin, A. W. *J. Polym. Sci., Polym. Chem. Edn.* 1975, **13**, 961
7 Wilson, D. in 'Polyimides' (Eds D. Wilson, H. D. Stenzenberger and P. M. Hergenrother), Chapman and Hall, New York, 1990, p. 189
8 Kim, S. C. and Brown, H. R. *J. Mater. Sci.* 1987, **22**, 2589
9 Morgan, R. J., Jurek, R. and Larive, D. E. *Am. Chem. Soc., Div. Polym. Sci. Eng.* 1990, **63**, 681
10 *Air Transport Magazine*, December 1990, p. 2
11 Boyd, J., Chang, G., Wells, W., Speak, S., Gerth, D. and Reck, B. *Int. SAMPE Symp.* 1991, **36**, 1217
12 Berry, J. P. *J. Appl. Phys.* 1963, **34**, 62
13 Whitney, J. M., Browning, C. E. and Hoogsteden, C. E. *J. Reinf. Plast. Compos.* 1987, **1**, 297
14 Keary, P. E., Ilcewicz, L. B., Shaar, C. and Trostle, J. *J. Compos. Mater.* 1985, **19**, 154
15 Ward, I. M. in 'Mechanical Properties of Solid Polymers', Wiley-Interscience, New York, 1985, p. 406
16 Russell, A. J. and Street, K. N. in 'Moisture and Temperature Effects on the Mixed Mode Delamination and Fracture of Unidirectional Graphite Epoxy', ASTM STP 876 (Ed. W. S. Johnson), ASTM, Philadelphia, 1985, p. 349
17 Davies, P., Cantwell, W., Moulin, C. and Kausch, H. H. *Compos. Sci. Technol.* 1989, **36**, 153
18 Hunston, D. L. *Compos. Technol. Rev.* 1984, **6** (4), 176
19 Yee, A. F. in 'Toughened Composites', ASTM STP 937 (Ed. N. J. Johnston), ASTM, Philadelphia, 1987, p. 383
20 Hashemi, S., Kinloch, A. J. and Williams, J. G. *J. Compos. Mater.* 1990, **24**, 918
21 Davies, P., Cantwell, W., Moulin, C. and Kausch, H. H. *Compos. Sci. Technol.* 1989, **36**, 153
22 Altstadt, V., Heckmann, W., Tesch, H., Weber, T. and Recker, H. G. in 'Plastics–Metals–Ceramics, SAMPE European Chapter' (Ed. H. L. Hornfeld), 1990, p. 267
23 Evans, R. E. and Masters, J. E. in 'Toughened Composites', ASTM STP 937 (Ed. N. J. Johnston), ASTM, Philadelphia, 1987, p. 413
24 Krieger, R. B. *Nat. SAMPE Symp.* 1985, **30**, 1570